

Research Article

Active Learning with a Noisy Annotator

Netta Shafir¹, Guy Hacohen¹, Daphna Weinshall¹¹. School of Computer Science and Engineering, Hebrew University of Jerusalem, Israel

Active Learning (AL) aims to reduce annotation costs by strategically selecting the most informative samples for labeling. However, most active learning methods struggle in the low-budget regime where only a few labeled examples are available. This issue becomes even more pronounced when annotators provide noisy labels. A common AL approach for the low- and mid-budget regimes focuses on maximizing the coverage of the labeled set across the entire dataset. We propose a novel framework called *Noise-Aware Active Sampling (NAS)* that extends existing greedy, coverage-based active learning strategies to handle noisy annotations. *NAS* identifies regions that remain uncovered due to the selection of noisy representatives and enables resampling from these areas. We introduce a simple yet effective noise filtering approach suitable for the low-budget regime, which leverages the inner mechanism of *NAS* and can be applied for noise filtering before model training. On multiple computer vision benchmarks, including CIFAR100 and ImageNet subsets, *NAS* significantly improves performance for standard active learning methods across different noise types and rates.

Corresponding author: Netta Shafir, netta.shafir@mail.huji.ac.il

1. Introduction

Deep learning typically relies on large amounts of annotated data. But while unlabeled data is often abundant, the annotation process can be both time-consuming and expensive. This challenge is particularly evident in fields like medical imaging, where annotations demand expert knowledge and are therefore costly. *Active Learning (AL)* offers a powerful approach to reducing annotation costs by prioritizing the most informative samples for model training.

In *pool-based active learning*, the challenge is formulated as a "best-subset" problem: Given a large pool \mathbb{U} of N unlabeled samples and an annotation budget $B \ll N$, the objective is to identify a subset $\mathbb{Q}^* \subset \mathbb{U}$, which is optimal in the following sense: After annotators label \mathbb{Q}^* , a model \mathcal{M} trained on \mathbb{Q}^* obtains the lowest generalization error compared to any other subset \mathbb{Q} of the same size B used for training \mathcal{M} . This

problem is NP-hard, even if all labels are available. Nevertheless, various heuristic strategies have been proposed that consistently outperform the baseline approach of random sampling.

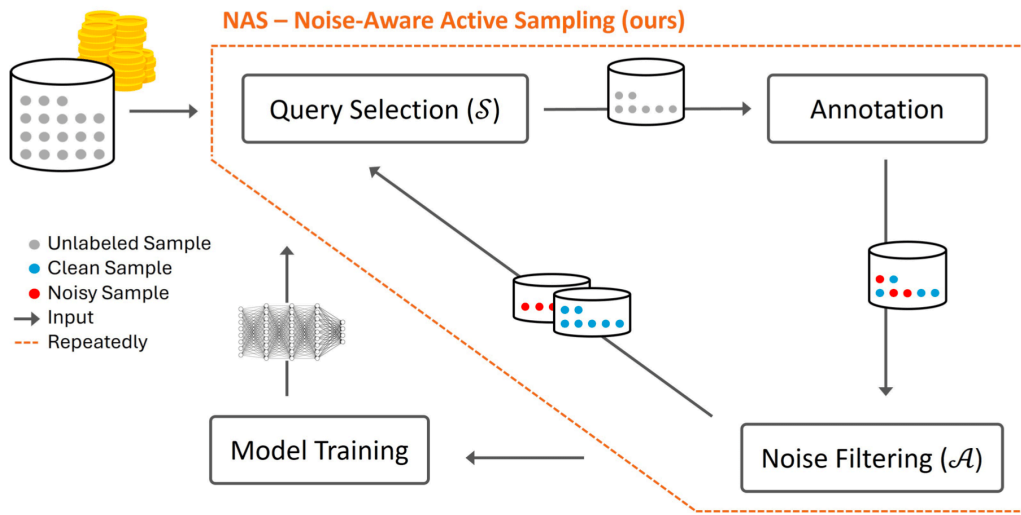


Figure 1. Overall visualization of our framework for Noise Aware Query Selection (NAS). NAS (illustrated with a dashed orange line) takes as input a query selection strategy \mathcal{S} and a noise-filtering algorithm \mathcal{A} . The framework alternates between selecting b samples using \mathcal{S} , sending these samples to the annotator, and filtering the noisy samples with \mathcal{A} before selecting the next set of samples.

Another important topic in this work is *Learning with Noisy Labels (LNL)*, which arises naturally due to errors in human and AI-generated annotations^[1]. Label noise becomes more likely as the annotator pool expands, such as in crowd-sourcing.

In this work, we focus on sample selection in AL and ask whether it is possible to design query selection strategies that account for noise when selecting samples for annotation. We propose a novel framework that extends existing query selection methods, particularly those based on sample distances, enabling them to intelligently account for label noise during sample selection.

Summary of Contributions

1. A query selection framework compatible with multiple state-of-the-art AL strategies, enhancing their performance in the presence of label noise (see Fig. 1).
2. Introduction of a simple yet effective noise filtering tool that performs well even with limited samples and integrates with the query selection framework.

3. Addressing the challenge of instance-dependent noise.

2. Background and Related Work

2.1. Active Learning

In most approaches within the pool-based active learning framework, the total annotation budget is allocated iteratively. In each iteration, a batch of B samples is selected for annotation. Beginning with an unlabeled set \mathbb{U} and a labeled set \mathbb{L} (which may or may not be initially empty), the process follows these steps:

1. **Query Selection** - Select a query $\mathbb{Q} \subseteq \mathbb{U}$ of size B using a strategy \mathcal{S} .
2. **Annotation** - Send \mathbb{Q} to the annotator to obtain labels, and update $\mathbb{L} = \mathbb{L} \cup \mathbb{Q}$ and $\mathbb{U} = \mathbb{U} \setminus \mathbb{Q}$.
3. **Model Training** - Train classifier \mathcal{M} using the labeled set \mathbb{L} (or with $\{\mathbb{L}, \mathbb{U}\}$ for semi-supervised learning).

Query selection strategies fall into two main categories: uncertainty-based and typicality-based, with diversity as another key consideration. Uncertainty-based strategies select samples where the model is least confident, based on its predictions for unlabeled data. This category includes methods like Margin^[2], Entropy^[3], and BADGE^[4].

Typicality-based strategies aim to identify a subset of "typical" samples in \mathbb{U} , under the rationale that a model trained on such a subset would generalize well. This family includes methods like k-medoids^[5], Typiclust^[6], ProbCover^[7], and MaxHerding^[8]. Typicality-based strategies rely on effective data representations. Recent methods like SimCLR^[9], MOCOv2^[10], and DINO^[11] have developed powerful self-supervised representations, enabling typicality-based strategies to perform well in complex domains, like natural images.

Previous works, such as^{[6][12]}, have shown that the annotation budget is a critical parameter in determining the most suitable strategy. Uncertainty-based strategies are more effective when the annotation budget is relatively high (hundreds of samples per class), whereas the low-budget regime (a few examples per class) is better suited for typicality-based strategies. A query selection strategy applied in an unsuitable budget regime may perform worse than random selection.

2.2. Learning with Noisy Labels

In settings with mislabeled data, approaches can be categorized into four families: *Robust Architecture*, *Robust Regularization*, *Robust Loss Design*, and *Sample Selection* (see review by Song et al.^[13]). Some have drawbacks, such as assuming a specific noise distribution. For instance, methods in the *Robust Architecture* family^{[14][15][16][17]} use a denoising layer to learn a noise transition matrix, later removed during inference. However, this assumes a noisy channel model based on class confusion and overlooks instance-dependent noise. Likewise, a few methods based on robust loss also assume such independence between label noise and input features^{[18][19]}.

Sample Selection Methods

LNL methods in the *Sample Selection* family aim to distinguish between mislabeled (noisy) and correctly labeled (clean) samples, allowing models to train primarily on clean data. Some methods exploit patterns in deep neural network (DNN) training dynamics. For example, Arpit et al.^[20]; Han et al.^[21] show that DNNs learn clean samples earlier than noisy ones, resulting in lower loss on clean samples during early training, before overfitting occurs. One method that leverages this is Area-Under-the-Margin (*AUM*)^[22], which measures the margin between the assigned label's logit and the highest other logit. The *AUM* score is computed by summing these margins over early training epochs. With appropriate early stopping, noisy samples tend to exhibit lower *AUM* scores. To establish a threshold for noise filtering, the method assigns a "fake" label $C + 1$ (where C is the number of classes) to a random subset of samples, treating them as an additional noisy class. The threshold is then determined based on the *AUM* scores of this fake class, and samples with *AUM* scores above the threshold are classified as clean.

Semi-Supervised Methods

The most effective LNL approaches are Semi-Supervised Learning (SSL) methods, which fall within the *Sample Selection* family. These methods identify clean and noisy samples and train an SSL model on all data, treating noisy samples as unlabeled. SSL methods have achieved state-of-the-art performance on standard LNL benchmarks. Examples include DivideMix^[23], UNICON^[24], ProMix^[25], and PGDF^[26]. However, in our experiments, we found that these methods performed poorly in the noisy low-budget setting, where most samples are unlabeled, and the labeled set contains noise.

2.3. Active Learning in the Presence of Label Noise

As Nuggehalli et al.^[27] have already noted, the setting of label noise in active learning has rarely been studied. Nevertheless, several papers address both topics of Active Learning and Label Noise. Gupta et al.^[17] examines the issue of noisy annotators in the active learning setting. Unlike us, they tackle this challenge by adding a denoising layer to the neural network rather than through an adjusted query selection strategy. Other works, such as^[28], assume access to multiple noisy annotators and a clean validation set, which simplifies the task of identifying noisy labels. Similarly, Zhang and Chaudhuri^[29]; Chen et al.^[30] assume the availability of a perfect oracle that always provides correct labels in addition to the noisy annotators. **Our work is orthogonal to these approaches** and can naturally integrate with improved architectures as well as the presence of multiple annotators.

The study by Nuggehalli et al.^[27] proposes a query selection method called *DIRECT*, which, like our approach, is adapted to handle noisy scenarios. However, *DIRECT* is specifically designed for cases involving noisy labels combined with extremely imbalanced data. Moreover, while *DIRECT* is better suited for high-budget scenarios, our method is tailored for low-budget settings.

Another category of work, such as^{[31][32]}, uses the term *Active Learning* in the context of data cleaning, where all data labels are available, and the goal is to identify suspicious samples for re-labeling by an oracle. In a sense, this setting is the opposite of ours. While this line of research can be viewed as a subset of the Learning with Noisy Labels (LNL) field incorporating active learning, our work is more appropriately described as a branch of Active Learning (AL) that addresses label noise.

Low-Budget AL in the Presence of Label Noise

Some typicality-based active learning methods aim to maximize the *coverage* of the labeled set, where a sample is considered to cover its neighbors in feature space. ProbCover^[2] formalized this objective as a greedy approximation of the *Maximum Coverage* problem, which is NP-hard. Typicality-based methods tend to excel in the low-budget regime by avoiding excessive sampling from the same regions of the data. However, label noise can be detrimental in this context. A noisy sample may be mistakenly treated as representative of its neighborhood, undermining the effectiveness of coverage.

3. Proposed Method

As summarized above, methods that are suitable for the low-budget regime of active learning may be detrimentally affected by label noise. Likewise, as DNN training requires substantial data in order to generalize, DNN-based noise-filtering methods are likely to fail in low-budget settings. Our method addresses these two challenges.

3.1. Noise Filtering Algorithms for Low Budget

Naive Method for Noise Filtering

Assuming we have a good representation of our data, where the distances between embeddings reflect the semantic distances between samples, a mislabeled sample would behave as an outlier and thus be detectable. Accordingly, we propose the following algorithm for noise filtering: Train a k-fold cross-validation linear model on the labeled data, and classify as noisy any sample for which fewer than half of the models agree with its given label. We refer to this noise-filtering method as *CrossValidation*.

DNN-based Noise Filtering

As noted earlier, DNN-based noise-filtering algorithms often fail in the low-budget regime (as well as the SOTA Semi-Supervised methods, like ProMix^[25]). To adapt such algorithms to this setting, we propose the following modification: Instead of training a DNN directly on the images, we extract representations for the images using a self-supervised pretrained model, and train a linear classifier on these embeddings. As a case study, we examine this adaptation in the context of the *AUM* method^[22], that was mentioned before. We introduce an adapted version of *AUM* for the low-budget setting, which we refer to as *LowBudgetAUM*. Most importantly, we compute the *AUM* score using a linear classifier on self-supervised representations instead of training a DNN on the images directly. Additionally, we determine an earlier stopping point and lower threshold, for the hyperparameters in the original paper are suboptimal in the low-budget regime (see Appendix C).

The empirical results presented in Fig. 2 demonstrate that while the original *AUM* method performs poorly in low-budget scenarios, *LowBudgetAUM* effectively predicts the noise rate while maintaining high recall and precision (when noise filtering is treated as a binary classification task).

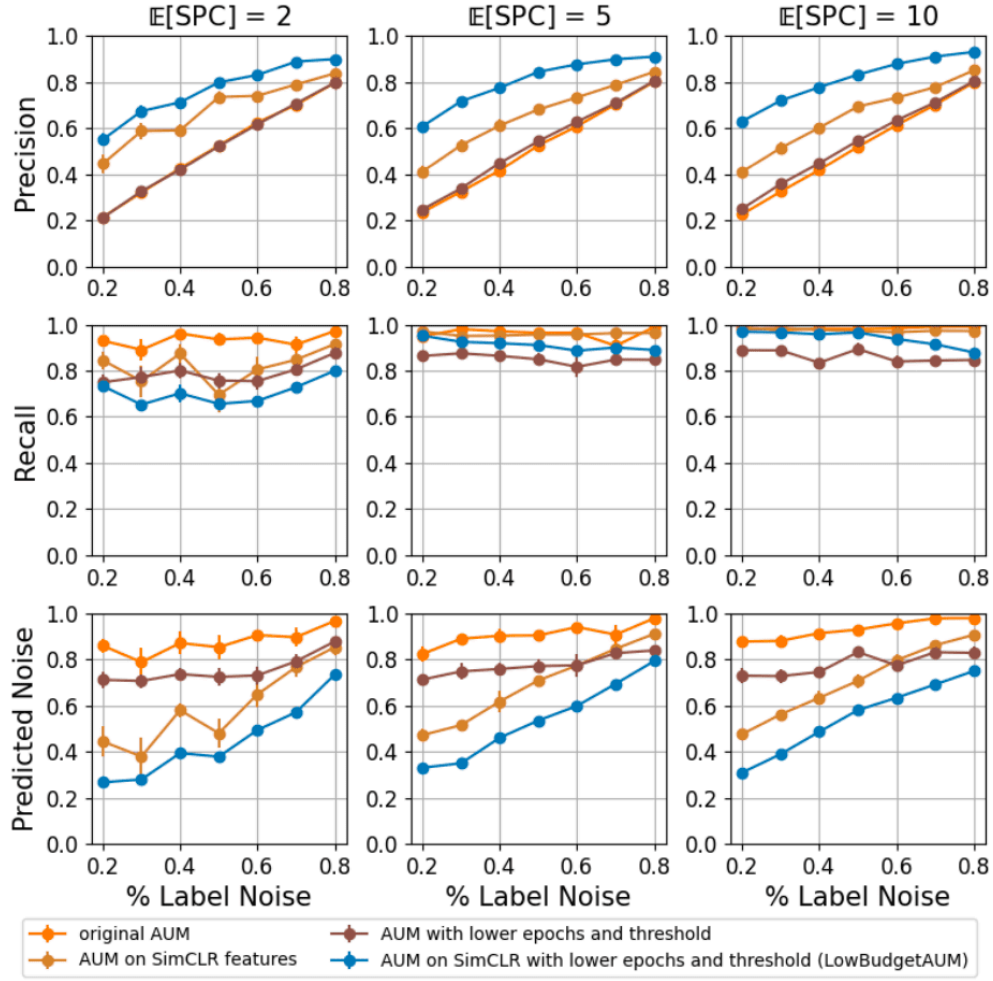


Figure 2. Performance of the AUM method in identifying mislabeled data selected by ProbCover in the low-budget regime on CIFAR100 with symmetric noise. Each column represents a different expected number of clean samples per class ($\mathbb{E}[\text{SPC}]$), with the budget given by $\frac{\mathbb{E}[\text{SPC}] \times C}{1 - \% \text{noise}}$. Rows show noise precision, recall, and predicted noise ratio. The orange line represents the original AUM, while the blue line represents *LowBudgetAUM*. Unlike AUM, which predicts most samples as noisy, *LowBudgetAUM* estimates noise rates more accurately—even with as few as two clean samples per class—while maintaining high precision and recall. Each point shows the mean and standard error across 10 repetitions.

3.2. NAS: Noise-Aware Strategy for Query Selection

Most state-of-the-art (SOTA) typicality-based query selection methods are greedy algorithms: in each iteration, samples are scored by their contribution to some objective function, and the sample with the

highest score is added to the labeled set. Our goal is to design a query selection strategy that greedily maximizes the same objective function while accounting for label noise. We propose the following framework: given a greedy, typicality-based query selection strategy \mathcal{S} , a noise-filtering algorithm for low-budget settings \mathcal{A} (e.g., LowBudgetAUM as discussed above), and an annotation budget B , the following cycle is executed:

1. Apply \mathcal{A} to the current labeled set \mathbb{L} to obtain a partition into a clean subset $\mathbb{L}_{\text{clean}}$ and a noisy subset $\mathbb{L}_{\text{noisy}}$.
2. Select a set \mathbb{Q} of size $b \ll B$ from the current unlabeled set \mathbb{U} using the strategy \mathcal{S} , considering only $\mathbb{L}_{\text{clean}}$ as the labeled set and ignoring $\mathbb{L}_{\text{noisy}}$.
3. Add \mathbb{Q} to \mathbb{L} and remove it from \mathbb{U} .

The cycle continues until the annotation budget B is exhausted. We refer to this method as **Noise-aware Active Sampling (NAS)**. If the strategy \mathcal{S} seeks to cover areas in the data, this meta-strategy needs to identify areas that remain uncovered after \mathcal{S} sampled from them, in the case the representative \mathcal{S} sampled turned out to be noisy. Psuedo-code for this method is provided below in Alg. 1.

Algorithm 1 NAS: Noise-aware Active Sampling

Input: unlabeled pool \mathbb{U} , initial labeled pool \mathbb{L}_{init} , query budget B , query selection strategy \mathcal{S} , noise filtering algorithm \mathcal{A} , a trained model \mathcal{M} (optional)

Output: a labeled set \mathbb{L}

$\mathbb{L} \leftarrow \mathbb{L}_{init}$

repeat

 Get a partition $(\mathbb{L}_{clean}, \mathbb{L}_{noisy}) = \mathcal{A}(\mathbb{L})$

if use_noise_dropout **then**

$\hat{q} = \frac{|\mathbb{L}_{noisy}|}{|\mathbb{L}|}$ *# the predicted noise ratio*

$\eta = 100 \times \max(\min(\hat{q}, 1 - \hat{q}), 0.1)$

 Randomly move $\eta\%$ from \mathbb{L}_{noisy} to \mathbb{L}_{clean}

end if

$b \leftarrow \text{number_of_classes}$

$\mathbb{Q} \leftarrow \mathcal{S}(\mathbb{L}_{clean}, \mathbb{U}, \mathcal{M}, b)$ *# select b samples with \mathcal{S}*

$\mathbb{L} \leftarrow \mathbb{L} \cup \mathbb{Q}$

$\mathbb{U} \leftarrow \mathbb{U} \setminus \mathbb{Q}$

until $|\mathbb{L}| = B$

return: \mathbb{L}

Algorithm 1. NAS: Noise-Aware Active Sampling

The Choice of b

Determining the hyperparameter b (the size of \mathbb{Q} at each iteration) involves a tradeoff: As $b \rightarrow 1$, our framework becomes more precise in correcting \mathcal{S} , but the computational complexity increases since more calls to \mathcal{A} are needed. Conversely, as $b \rightarrow B$, the runtime decreases, but the framework behaves more similarly to \mathcal{S} . In all our experiments, we set $b = C$, where C is the number of classes in the dataset. In the special case of using an ideal noise-filtering algorithm (one that makes no mistakes), we set¹ $b = 1$. The complexity of the algorithm is dominated by the run-time of \mathcal{S} and \mathcal{A} , and is given by $T_S + \frac{B}{b} \cdot T_A$.

ProbCover as a Working Example

ProbCover^[7] is a SOTA strategy for active learning in the low-budget regime. Like other typicality-based strategies, it aims to maximize the coverage of \mathbb{L} . A sample x is considered to cover all samples in $B_{(d,\delta)}(x)$, where $B_{(d,\delta)}(x)$ is a ball around x with radius $\delta > 0$, defined with respect to some metric $d(\cdot, \cdot)$. Both δ and metric d are hyperparameters of *ProbCover*. Initially, *ProbCover* constructs a directed graph G ,

where each vertex represents a sample, and there is an edge between two vertices (x, x') if and only if $x' \in B_{(d,\delta)}(x)$. At each iteration, *ProbCover* adds to \mathbb{Q} the sample $x \in \mathbb{U}$ with the highest out-degree in G , and then removes all incoming edges to the samples in $B_{(d,\delta)}(x)$. This step is crucial for preventing excessive sampling from the same area, thereby maintaining high coverage of \mathbb{L} . The coverage of \mathbb{L} , in this context, is the union of all the balls $B_{(d,\delta)}(x)$ for samples in \mathbb{L} , i.e., $\text{coverage}(\mathbb{L}) \triangleq B_{(d,\delta)}(\mathbb{L}) \triangleq \bigcup_{x \in \mathbb{L}} B_{(d,\delta)}(x)$.

Given *ProbCover* as the selection strategy \mathcal{S} , our framework functions as follows: After every b query selections and obtaining a partition $(\mathbb{L}_{\text{clean}}, \mathbb{L}_{\text{noisy}})$, we remove all edges in $B_{(d,\delta)}(\mathbb{L}_{\text{clean}})$ as well as the outgoing edges of the noisy samples. The latter step is essential to prevent re-selecting the noisy samples themselves. This approach ensures that the density of an area — and consequently the query selection score — remains high until we confirm that a clean sample has been selected from it. In Appendix A, we present the pseudo-code for the case where *NAS* employs *ProbCover* as \mathcal{S} , which we refer to as **Noise-Aware ProbCover (NPC)**.

Updating *ProbCover*'s radius δ

δ is a crucial hyperparameter of *ProbCover*, and Bae et al.^[8] have demonstrated its high sensitivity to this parameter. The authors of *ProbCover* proposed an automatic algorithm for determining δ without requiring a validation set (as the existence of a validation set is often unrealistic in low-budget scenarios). However, this approach does not guarantee optimal results.

In our experiments, we observed an additional issue related to the radius δ : during the selection process, the maximal degree in the graph diminishes, until the graph eventually becomes empty. When this occurs, we update δ using the following policy: (i) Construct a series of graphs G_δ , each corresponding to a different δ value. (ii) Remove from these graphs the samples already selected by *ProbCover* and their associated edges in $B_{(d,\delta)}$ balls. (iii) Choose the δ corresponding to the graph with the highest maximal degree.

The rationale behind this policy is as follows: The maximal degree, as a function of δ , is concave within the range $[0, \delta_{\text{init}}]$, where δ_{init} represents the value of δ previously used by *ProbCover*. As $\delta \rightarrow 0$, the graph's maximal degree approaches zero, even before removing samples. Similarly, as $\delta \rightarrow \delta_{\text{init}}$, the graph becomes empty by definition. Fig. 3 illustrates this behavior. The value of δ that maximizes the graph's maximal degree, while considering the already sampled points, yields the most informative distribution for subsequent query selections.

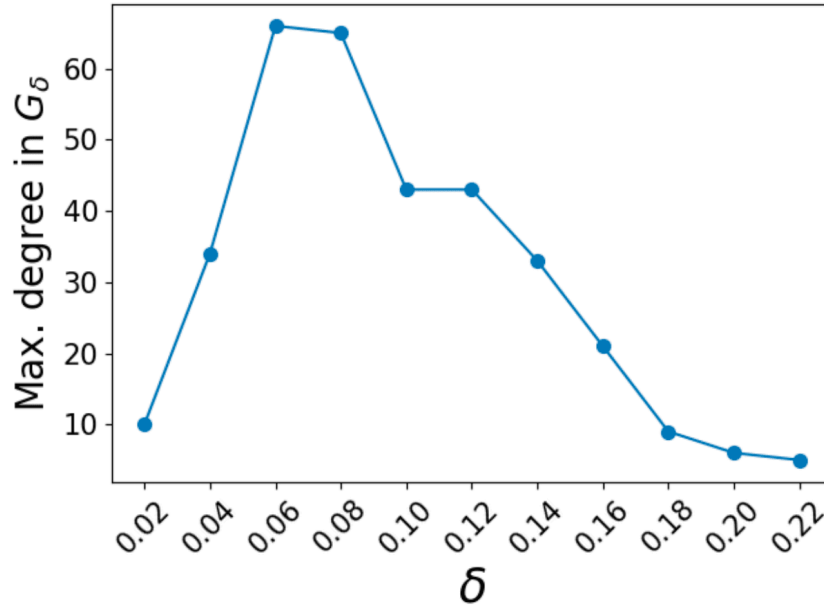


Figure 3. The maximal degree in graphs G_δ of CIFAR100, after removing 3200 samples picked by ProbCover with $\delta = 0.22$, as a function of δ . On this range, this function is generally concave, regardlessly to the number of samples ProbCover picked.

Adapting NPC to Instance-Dependent Noise

The above adaptation is well-suited for scenarios where the label noise is conditionally independent of the sample's features, such as the symmetric and asymmetric label noise cases described in^[33]. However, in many real-world scenarios, this independence assumption does not hold. When the annotator is a human or even an AI model, some samples may be inherently "harder" to label than others, leading to a higher probability of these samples being mislabeled. Furthermore, such "harder" samples tend to cluster in the feature space of a Self-Supervised Learning (SSL) model, creating "noise clusters"—regions where noisy samples are concentrated. An example of this phenomenon is provided in Appendix B.

To address this scenario, we adapt *NPC* as follows: *ProbCover* can be viewed as initializing a weighted graph where all edges have an initial weight of 1. When a sample is selected, the algorithm reduces the weights of edges in the $B_{(d,\delta)}$ ball around that sample to 0. The out-degree of a sample is then computed as the sum of the weights of its outgoing edges. In our adaptation for instance-dependent noise, after obtaining predictions from the noise-filtering algorithm, we reweigh the edges. Specifically, for samples in $B_{(d,\delta)}(\mathbb{L}_{\text{noisy}})$, we set the weights of their incoming edges to $1 - \hat{q}$, where $\hat{q} = \frac{|\mathbb{L}_{\text{noisy}}|}{|\mathbb{L}|}$ represents the

estimated noise rate. These modified weights reflect the motivation to sample from noisy regions as a decreasing function of the estimated noise rate. This reweighing step thus balances the trade-off between achieving sufficient coverage of the data and avoiding excessive sampling from noisy regions. We refer to this version of the algorithm as *Weighted NPC*.

Using Noise Dropout

Fig. 2 demonstrates that *LowBudgetAUM* performs well in the low-budget regime. Nevertheless, its performance is influenced by the distribution of samples in the labeled set. In some cases of high noise rates combined with specific distributions of the labeled data, we observed that *LowBudgetAUM* could predict noise rates significantly higher than the actual noise rates.

To address these pathological cases, we utilized the following solution: we define $\eta = \max(\min(\hat{q}, 1 - \hat{q}), 0.1)$, where \hat{q} is the predicted noise rate. We then randomly select $\eta\%$ of the samples that *LowBudgetAUM* predicts to be noisy and treat them as if they were clean samples in the next iteration². This addition to *NAS* was shown to resolve these pathological cases effectively. In Appendix F, we demonstrate that noise dropout does not harm performance, even when applied in scenarios with low predicted noise rates.

4. Empirical Evaluation

We evaluated two training frameworks:

1. A fully supervised framework, in which we trained a ResNet-18 on the labeled samples.
2. A linear model trained using the labeled samples, on features extracted from a self-supervised model, pretrained on the unlabeled dataset.
3. A linear model trained using the labeled samples, on features extracted from a self-supervised model, pretrained on the unlabeled dataset.

Both frameworks were evaluated with the symmetric noise scenario. For the other scenarios — asymmetric noise, real-world noise, and most of the ablation study — only framework 2 was evaluated, for it easier to train and usually outperforms framework 1 in the low-budget regime. The implementation details are given in the Appendix C. In both frameworks and across all active learning (AL) strategies, noisy samples were filtered *prior to the supervised training step* using either *LowBudgetAUM* or *CrossValidation*, depending on the noise-filter that *NAS* used. The model was then trained exclusively on the clean samples, a standard approach for learning with label noise (see 2.2). This preprocessing step improved the

performance of all query selection methods. Nevertheless, as demonstrated in the ablation study, this filtering process is not the sole factor contributing to the advantage of using NAS.

4.1. Methodology

Synthetic Noise

We used two benchmark datasets: (i) CIFAR100^[34], and (ii) ImageNet-50^[35]. ImageNet-50 is a subset of ImageNet^[36], containing 50 classes, 64K train images, and 2,500 test images. Different levels of symmetric and asymmetric label noise were explored. Symmetric (or uniform) noise was introduced by randomly selecting a subset of samples from the dataset and uniformly replacing their labels with other labels at random. For the asymmetric (or label-dependent) noise scenario, prior work^{[37][19][13]} modeled the noise as a transition matrix T , where $T_{ij} = P(\tilde{y} = j \mid y = i)$ represents the probability of a sample having a noisy label \tilde{y} given that its true label is y . For a specified noise ratio, T determines both the proportion of noisy samples in each class and the assignment of incorrect labels. To simulate a challenging transition matrix, we trained a ResNet-18 on the full dataset for 10 epochs, generated a confusion matrix based on the network's predictions on the test set, and normalized each row of the confusion matrix to produce the transition matrix T .

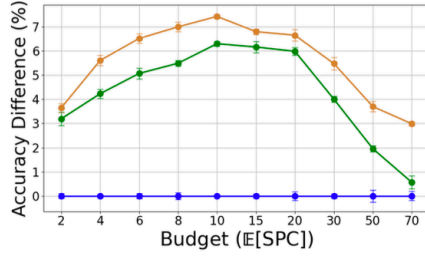
Real-World Noisy Datasets

We tested our method on the real-world noisy dataset of CIFAR100N^[38], which contains the images of CIFAR100 with human-annotated labels and includes 40.2% noise, and on the dataset Clothing1M^[39] which contains clothing images with noisy labels collected from online shopping websites. On these dataset, we compared *ProbCover* to *NPC* — our method NAS when using ProbCover as \mathcal{S} — and to *Weighted NPC*.

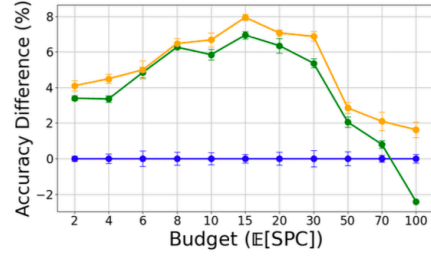
Self-Supervised Representations

For pretrained features, we used SimCLR^[9] for CIFAR100 and CIFAR100N and DINOv2^[11] for ImageNet-50. These embeddings used us as feature spaces for the coverage-based AL strategy \mathcal{S} and the low-budget noise filter algorithm \mathcal{A} , as well as feature spaces in which we trained the linear classifier in framework 2. In Appendix H, we examine additional feature spaces, demonstrating the robustness of our framework to different representations.

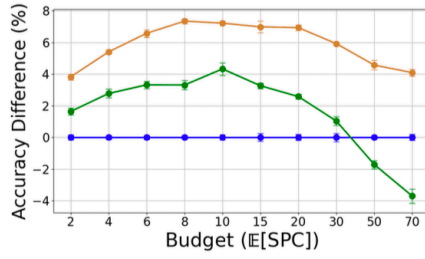
4.2. Results



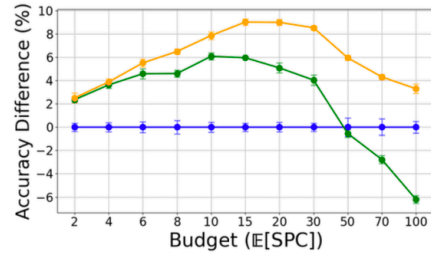
(a) CIFAR100, 20% Noise



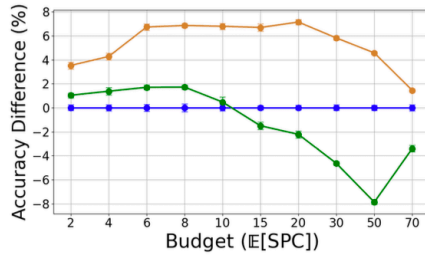
(b) ImageNet-50, 20% Noise



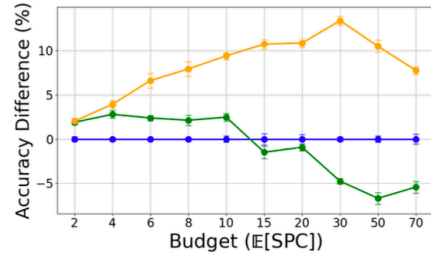
(c) CIFAR100, 50% Noise



(d) ImageNet-50, 50% Noise



(e) CIFAR100, 80% Noise



(f) ImageNet-50, 80% Noise

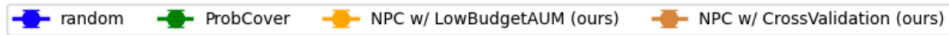


Figure 4. Framework 1, results on CIFAR100 and ImageNet-50 with varying symmetric noise levels. The y-axis shows the mean accuracy difference from random query selection. A ResNet-18 model is trained in a fully supervised manner.

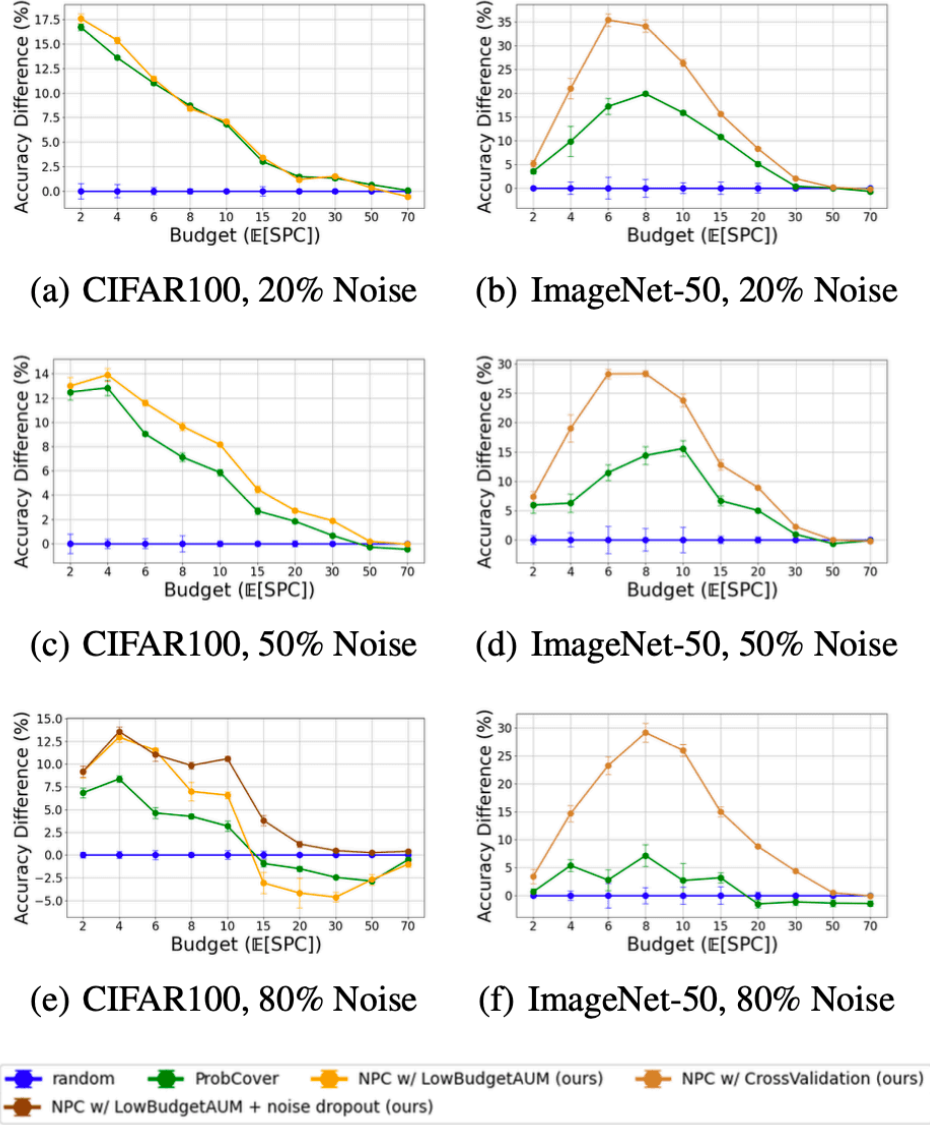


Figure 5. Framework 2, see caption of Fig. 4. Here we evaluate a linear model trained on self-supervised pretrained features.

Figures 4 and 5 show the results for the symmetric noise scenario under training frameworks 1 and 2, respectively. The y-axis in all the plots presents the difference between the mean accuracy achieved by each query selection method and the mean accuracy obtained by training a similar model using random query selection, along with the Standard Error (STE) for 5 repetitions (all experiments in this paper repeated 5 times). The x-axis counts the annotation budget, in units of expected clean samples per class ($\mathbb{E}[\text{SPC}]$), where the budget in each point equals $\frac{\mathbb{E}[\text{SPC}] \times C}{1 - \% \text{noise}}$. Fig. 6 shows the results for asymmetric noise, and Fig. 7 presents the results for CIFAR100N. Results for Clothing1M can be found in Appendix E. To

demonstrate robustness to the noise-filtering algorithm \mathcal{A} , in figures 4 and 5 under the symmetric noise scenario, we vary \mathcal{A} between subplots. In Framework 1, *CrossValidation* is employed when training with CIFAR100, while *LowBudgetAUM* is employed when training with ImageNet-50. In Framework 2, the selection of the noise-filtering method is reversed. In Appendix G, we introduce additional noise-filtering algorithms tailored to the low-budget regime and show that *NPC* outperforms *ProbCover* regardless of the noise-filtering algorithm used.

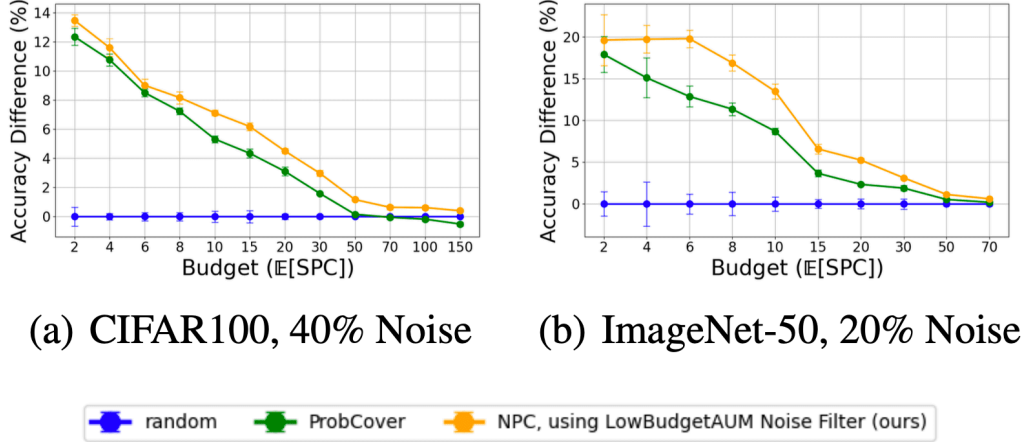


Figure 6. Results given different levels of asymmetric noise.

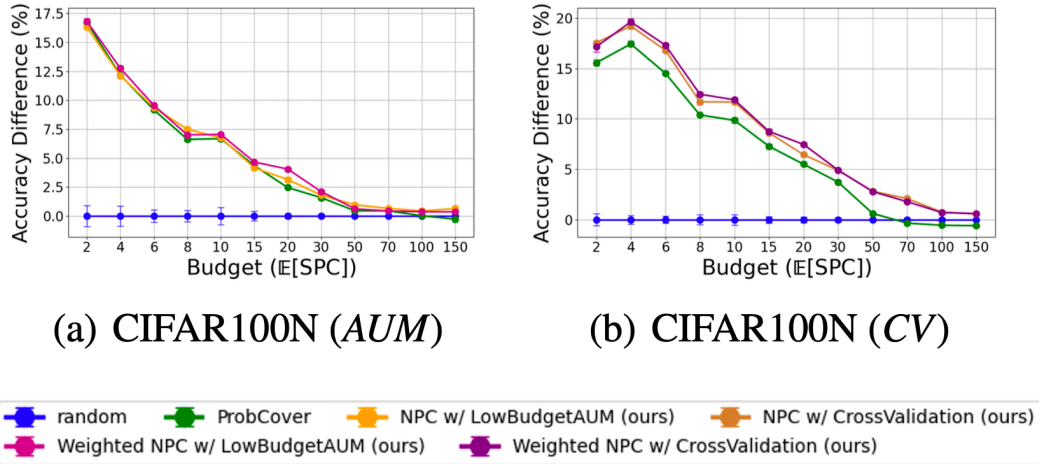


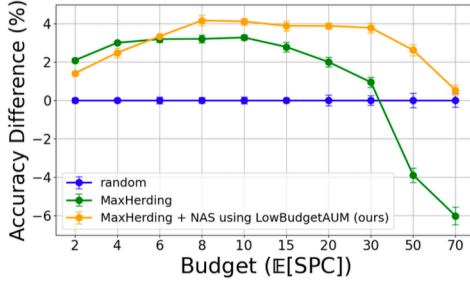
Figure 7. Results on CIFAR100N, where noise filtering is done with *LowBudgetAUM* in (a) and *CrossValidation* in (b). Note that generally the *Weighted NPC* outperforms the naive *ProbCover*, and also the regular *NPC*, with a small margin.

Comparison to Other AL Methods

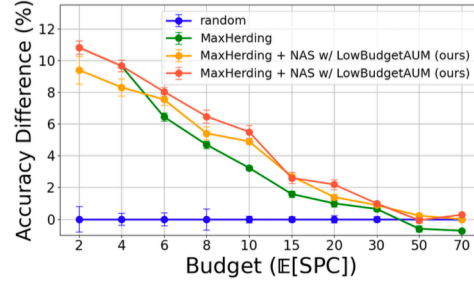
As mentioned in the Introduction, Nuggehalli et al.^[27] propose a query selection method called *DIRECT*, designed to handle noisy scenarios. However, its focus on imbalanced data and high-budget settings makes it less directly comparable to our *NAS*. Nonetheless, we provide a comparison with *DIRECT* in Appendix I.

Different Greedy AL Strategies

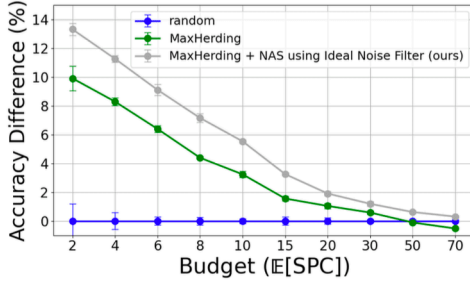
NAS enhances any greedy, coverage-oriented AL strategy \mathcal{S} , with the key comparison being between \mathcal{S} and its *NAS*-adjusted version. Our evaluations primarily used *ProbCover* as \mathcal{S} for its simplicity and effectiveness. Here, we assess *NAS* with other strategies, specifically *Coreset*^[40] and *MaxHerding*^[8], which are also greedy and structure-based. Tested on CIFAR100 with 50% symmetric noise, our framework consistently improved performance, demonstrating its generality (Fig. 8). Additional *MaxHerding* results appear in Appendix D. Figure 8(b) examines initially using *MaxHerding* and switching to *MaxHerding* + *NAS* after an initial budget has been reached. This approach makes sense because *LowBudgetAUM* may not perform optimally when the budget is extremely low. Thus, one might consider incorporating *NAS* only after a few iterations of query selection.



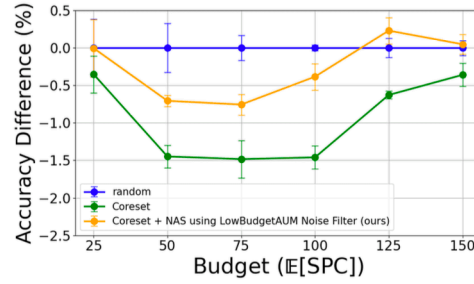
(a) MaxHerdling



(b) MaxHerdling



(c) MaxHerdling



(d) Coreset

Figure 8. Results of enhancing two additional AL strategies with NAS, on CIFAR100 with 50% symmetric noise. (a)–(c) Compare *MaxHerdling* with *Maxherding* + NAS when (a) use training framework 1, (b) uses framework 2 and (c) use framework 2 with ideal noise filter. (d) compares *Coreset* with *Coreset* + NAS using framework 2. In (a)–(c) a noise filtering was applied before training, and in (d) the training was conducted using all labeled samples without filtering out noisy ones. The dark orange line in (b) is *MaxHerdling* until budget equals $4 \mathbb{E}[\text{SPC}]$, followed by *MaxHerdling* + NAS.

4.3. Ablation Study

Contribution of the Noise Filter

To isolate the dependence of the improved performance of NAS on the quality of the noise filtering method, we replaced the filtering module with an *ideal Noise Filter* capable of perfectly detecting noisy samples. This ideal filter was used both as an input to NAS and to remove noisy labels prior to model training across all strategies. The results in Fig. 9 demonstrate that NAS continues to enhance the performance of *ProbCover*, confirming that the observed improvement is not an artifact of the *CrossValidation* or *LowBudgetAUM* algorithms.

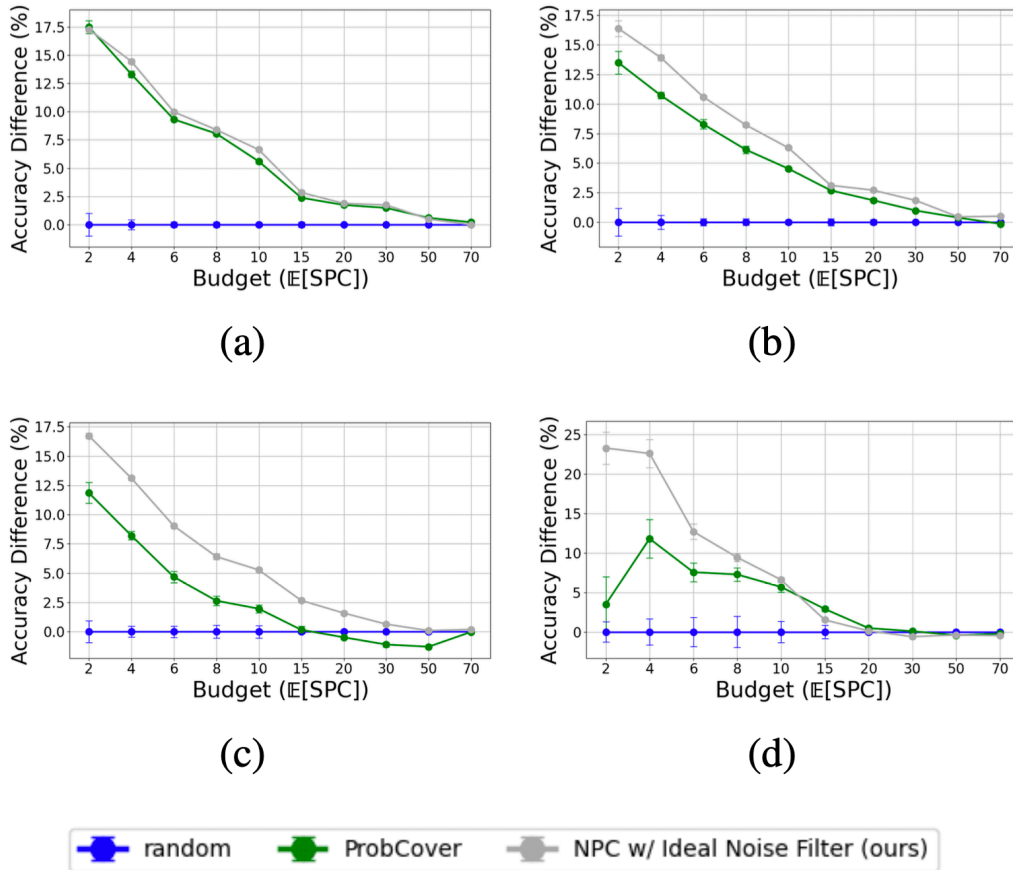


Figure 9. Results when using an ideal noise filter. (a-c) CIFAR100 with 20%, 50% and 80% symmetric noise; (d) ImageNet-50 with 50% symmetric noise, when using framework 2 for training.

Fixing the Number of Samples

As previously mentioned, training involved cleaning the noisy samples beforehand. However, this approach can lead to small variations in the exact number of training samples between methods, even when the labeled sets have equal noise rates (e.g., in the symmetric noise setting) and the same noise-filtering algorithm is used. To isolate the dependence of the improved performance of NAS on this component, we fixed an equal number of training samples across all AL strategies. This was accomplished in one of two ways: (i) All labeled samples were used for training. (ii) *LowBudgetAUM* was applied before training and the top $p\%$ most confident samples based on the *AUM* score were selected. Here, p was determined by the *LowBudgetAUM* prediction of the noise level after applying the NAS strategy. The absolute test accuracies were lower in this settings, especially when training using all the samples. Not

surprisingly, since NAS allowed a more accurate selection of fraction p , the gap between *ProbCover* and *NPC* narrowed. Still, *NPC* improved performance over *ProbCover* with fixed p in most cases, see Fig. 10.

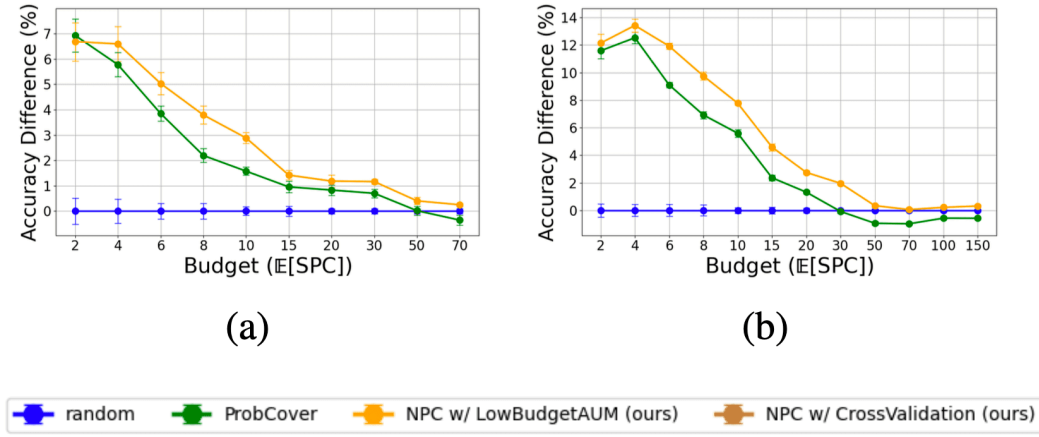


Figure 10. Framework 2, results when fixing an equal number of samples, on CIFAR100 with 50% symmetric noise. (a) Training on all samples. (b) Training on the $p\%$ most confident samples w.r.t the AUM score; p was determined using the noise estimation of the *LowBudgetAUM* when using *NPC*.

The contribution of δ Updating

As shown in Fig. 11, the δ update policy described above significantly improved performance in the fully supervised setting (Framework 1), while its impact in the linear model setting (Framework 2) was mostly negligible, with a slight negative effect observed for the largest budget. This component of *NPC* is not directly related to the noisy label scenario but rather addresses a limitation in the *ProbCover* algorithm, which serves as our test-bed AL method for evaluating NAS. Selecting an appropriate δ value and dynamically updating it during the execution of *ProbCover* remains an open question for future work.

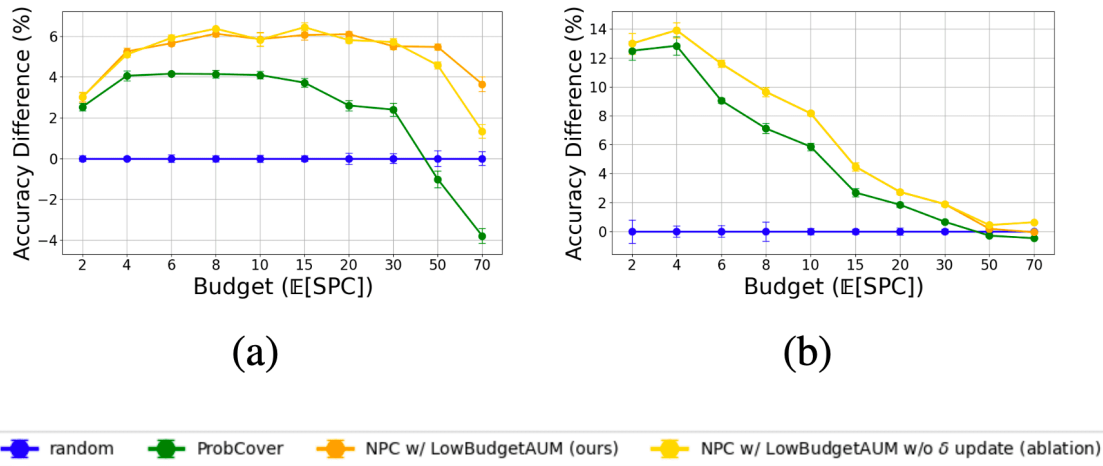


Figure 11. Accuracy improvement results for CIFAR100 with 50% symmetric noise are presented, where (a) corresponds to the fully supervised model (Framework 1) and (b) represents a linear model trained on pretrained self-supervised features (Framework 2).

5. Summary and Discussion

We investigated the problem of active learning in the presence of label noise and proposed a framework that extends query selection strategies, particularly greedy coverage-oriented approaches, by incorporating noise-awareness through a low-budget noise-filtering algorithm. Our framework identifies regions in the data that remain uncovered due to noisy representatives being selected by the underlying strategy, and resamples from these regions.

Two key assumptions suggest that noisy samples should not be sent back to the annotator: (i) the pool of unlabeled data contains enough similar samples to serve as alternatives, and (ii) the same annotator is likely to repeat a labeling error on a sample they previously mislabeled. In terms of the **exploration-exploitation tradeoff**, this approach prioritizes **exploration** of new samples over **exploitation** of existing data.

However, in scenarios involving multiple annotators^[41], or that we have a strong prior about the probability of the annotator to change her mind^{[42][43]}, the second assumption becomes less compelling, and resampling previously mislabeled samples could prove beneficial. This opens up new directions for future research, particularly in settings where annotator diversity can be utilized to mitigate label noise effectively.

Appendix A. Pseudo Code for NPC (ProbCover + NAS)

In this paper, we propose the NAS algorithm that derives a strategy \mathcal{S} for query selection, though most of our results present NAS using ProbCover as \mathcal{S} . Algorithm 2 presents the pseudo-code for this ProbCover + NAS combination, which we refer to as **Noise-Aware ProbCover (NPC)**.

Algorithm 2 NPC: Noise-Aware ProbCover

Input: unlabeled pool \mathbb{U} , initial labeled pool \mathbb{L}_{init} (typically \emptyset), query budget B , noise filtering algorithm \mathcal{A} , distance metric $d(\cdot, \cdot)$, ball radius δ_{init}
Output: a labeled set \mathbb{L}

$\mathbb{L} \leftarrow \mathbb{L}_{init}$
 $\delta \leftarrow \delta_{init}$
repeat
 $G_\delta \leftarrow (V = \mathbb{U} \cup \mathbb{L}, E = \{(x, x') : x' \in B_{(d, \delta)}(x)\}, W = 1^{|E|})$
 Get a partition $(\mathbb{L}_{clean}, \mathbb{L}_{noisy}) = \mathcal{A}(\mathbb{L})$
if use_noise_dropout **then**
 $\hat{q} = \frac{|\mathbb{L}_{noisy}|}{|\mathbb{L}|}$ # \hat{q} is the predicted noise ratio
 $\eta = 100 \times \max(\min(\hat{q}, 1 - \hat{q}), 0.1)$
 Randomly move $\eta\%$ from \mathbb{L}_{noisy} to \mathbb{L}_{clean}
end if
for $z \in \mathbb{L}_{clean}$ **do**
 Set $W(e) \leftarrow 0$ for all $e \in \{(x', x) \in E : (z, x) \in E\}$ # Zero the weights of all incoming edges to covered samples
end for
for $z \in \mathbb{L}_{noisy}$ **do**
 Set $W(e) \leftarrow 0$ for all $e \in \{(z, x) \in E\}$
 Set $W(e) \leftarrow 1$ for all $e \in \{(x', x) \in E : (z, x) \in E\}$ # Or $W(e) \leftarrow (1 - \frac{|\mathbb{L}_{noisy}|}{|\mathbb{L}|})$ as in *Weighted NPC* (see 3.2)
end for
 $\mathbb{Q} \leftarrow \emptyset$
 $b \leftarrow \text{number_of_classes}$
for $i \in [1, \dots, b]$ **do**
 Set $\text{ODR}(x) \leftarrow \sum_{e=(x, x')} W(e)$ for all $x \in \mathbb{U}$ # The Out-Degree rank is the sum of outgoing edges' weights
 $x_{max} \leftarrow \arg\max_{x \in \mathbb{U}} \text{ODR}(x)$
 $\mathbb{Q} \leftarrow \mathbb{Q} \cup \{x_{max}\}$
 Set $W(e) \leftarrow 0$ for all $e \in \{(x', x) \in E : (x_{max}, x) \in E\}$
end for
 $\mathbb{L} \leftarrow \mathbb{L} \cup \mathbb{Q}$
 $\mathbb{U} \leftarrow \mathbb{U} \setminus \mathbb{Q}$
if $\max_x \text{ODR}(x) \leq 1$ **then** # So G_δ is empty from edges which are not loops
for a given δ' **do**
 Define $G_{\delta'} = (V = \mathbb{U} \cup \mathbb{L}, E = \{(x, x') : x' \in B_{(d, \delta')}(x)\})$
 Remove from $G_{\delta'}$ the edges $\{(x', x) \in E : (z, x) \in E\}$ for all $z \in \mathbb{L}$
 Define $\text{ODR}_{\delta'}(x)$ as the Out-Degree rank of x in $G_{\delta'}$
end for
 Update $\delta \leftarrow \arg\max_{\delta'} [\max_x \text{ODR}_{\delta'}(x)]$
end if
until $|\mathbb{L}| = B$
return: \mathbb{L}

Algorithm 2. NPC: Noise-Aware ProbCover

Appendix B. Noise Clusters in CIFAR100N

In Section 3.2, we describe the phenomenon of noise clusters in datasets with instance-dependent noise. To investigate this phenomenon, we conducted the following experiment: Using SimCLR representations of CIFAR100, we imported the labels from CIFAR100N^[38], which contain human annotations for CIFAR100 with a label noise rate of 40.2%. We assigned pseudo-label 1 to correctly labeled samples and pseudo-label 0 to noisy samples in CIFAR100N. We then trained a 20-NN classifier on the SimCLR features and the pseudo-labels. The classifier achieved a training accuracy of ≈ 0.65 , significantly higher than the expected accuracy of ≈ 0.5 if the noise were uniformly distributed across samples.

To visualize the noise clusters in CIFAR100N, we present a t-SNE visualization in Figure 12 (based on the SimCLR features of CIFAR100), where noisy samples are colored red, and clean samples are colored black. For comparison, we include a similar visualization for CIFAR100 with a symmetric noise rate of 40.2%. The stark difference between the two plots highlights the presence of areas in CIFAR100N where noisy samples are concentrated, forming distinct noise clusters.

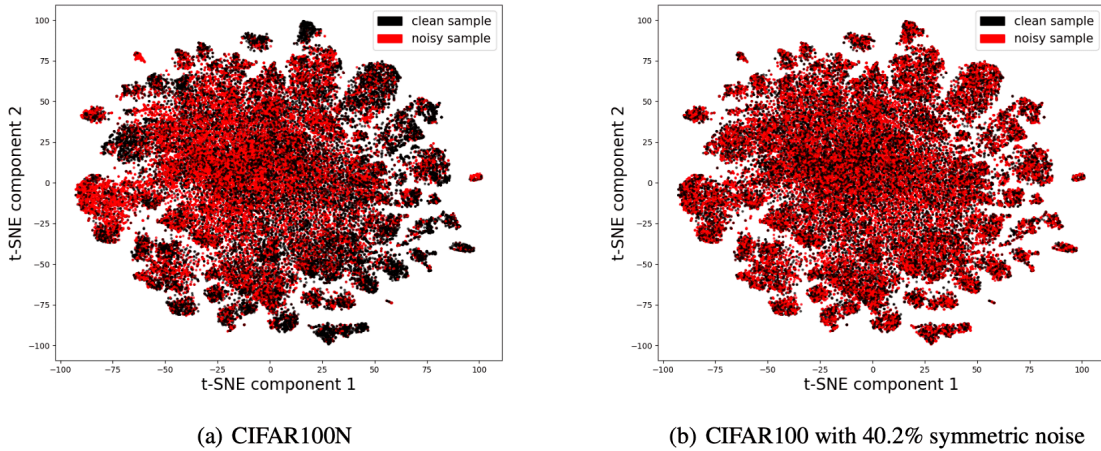


Figure 12. A t-SNE visualization of noisy and clean samples in (a) CIFAR100N and (b) CIFAR100 with a comparable symmetric noise rate. Noisy samples are shown in red, while clean samples are shown in black.

In the context of active learning, the presence of noise clusters creates a tension between two conflicting goals: (i) achieving sufficient coverage of the data and (ii) The risk of "getting bogged down in the noise mud" by repeatedly sampling from noisy areas while seeking clean samples, thus wasting a significant portion of the annotation budget. To address this challenge, in cases where there is a strong dependence

between a sample's features and its probability of being mislabeled, we propose *Weighted NPC*, as described in Section 3.2.

Appendix C. Implementation Details

Active Learning methods

Our experimental setup is based on the codebase of^[44], after adjusting it to the noise scenario. The implementation of the *Coreset*^[40] was taken from that codebase. The implementation of *ProbCover* algorithm was sourced from the official repository <https://github.com/avihu11/TypiClust>. As for *MaxHerdin*^[8], we used an implementation that was sent to us by the paper's authors.

For the hyperparameter δ in *ProbCover*, we used the values specified in the original paper.

Noise-Filtering methods

For *CrossValidation*, we used three folds and trained a multi-class logistic regression model for each fold pair. As for *LowBudgetAUM*, in the original *AUM* paper, the early stopping point is fixed at 150 epochs, and the threshold is set at the 99th percentile *AUM* score of the fake class. However, in the low-budget regime, these hyperparameters are suboptimal: overfitting occurs earlier, requiring an earlier stopping point, and the 99th percentile threshold is often a single sample, which might achieve a high *AUM* score by chance. Therefore, for *LowBudgetAUM*, we set the early stopping to 40 epochs, and determined the threshold above which samples are considered clean to be the 80th percentile of the fake-class *AUM* score.

In addition, the samples from the fake-class are randomly sampled from the unlabeled dataset, in contrast to the original *AUM* method that set aside some of the labeled dataset for this purpose, and consequently the original *AUM* must be executed multiple times for all samples in the dataset will receive predictions.

Supervised Learning Training (Framework 1)

For CIFAR100 and all noise levels, we utilized a ResNet-18 architecture trained for 200 epochs. Our optimization strategy involved using an SGD optimizer with a Nesterov momentum of 0.9, weight decay set to 0.0003, and cosine learning rate scheduling starting at a base rate of 0.025. Training was performed with a batch size of 100 examples, and horizontal flips were applied for data augmentation.

For ImageNet-50, the only changes were that the training batch size was 50, and the base learning rate was 0.01.

As for the linear model in Framework 2, the hyperparameters were the same, except for the number of training epochs, which was set to 500.

Appendix D. Additional Results for *MaxHerding*

MaxHerding^[8] is a state-of-the-art (SOTA) algorithm for active learning in the low-budget regime. The paper introduces a generalized definition of coverage that depends on a kernel function, with certain choices of this function recovering the *ProbCover* algorithm. Like *ProbCover*, *MaxHerding* also has a hyperparameter σ (the lengthscale of the kernel function), but the authors show that *MaxHerding* with a Gaussian kernel is significantly less sensitive to σ than *ProbCover* is sensitive to δ^3 . Since *MaxHerding* is both greedy and coverage-based, it can also serve as the query selection strategy \mathcal{S} in the NAS framework.

Here, we present additional results for *MaxHerding* on CIFAR100 under different levels of symmetric noise, comparing it with *MaxHerding* + NAS. Figures 14 and 15 show the results using training frameworks 2 and 1, respectively.

Figure 14(b) explores the strategy of initially using *MaxHerding* and later switching to *MaxHerding* + NAS after an initial budget has been reached. This approach makes sense because *LowBudgetAUM* may not perform optimally when the budget is extremely low. Thus, one might consider incorporating NAS only after a few iterations of query selection.

Fig. 13 show results when using an ideal noise filter, both for query selection in NAS and for noise filtering before training. Fig 14 shows results when the noise filtering algorithm is *LowBudgetAUM*.

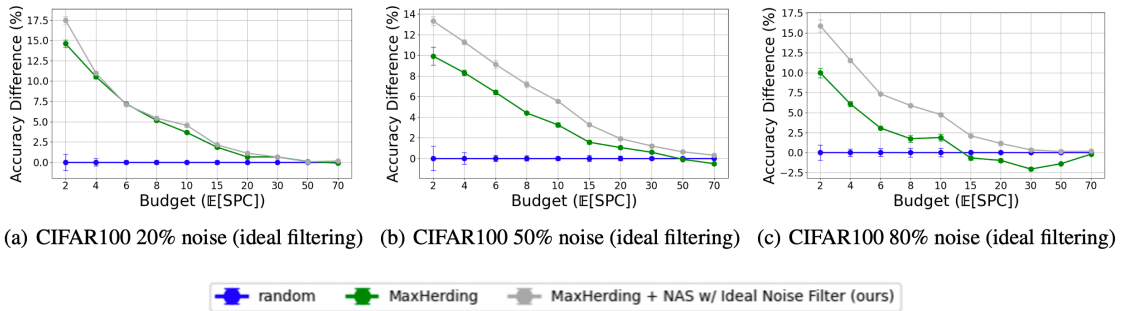


Figure 13. Results of *MaxHerding* compared to *MaxHerding*+ NAS when using Ideal noise filter . The training is done by framework 2.

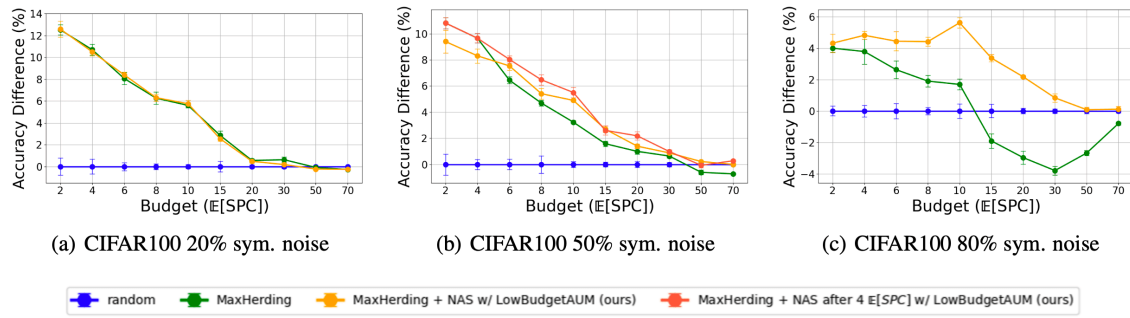


Figure 14. Results of *MaxHerdling* compared to *MaxHerdling* + NAS when using training framework 2.

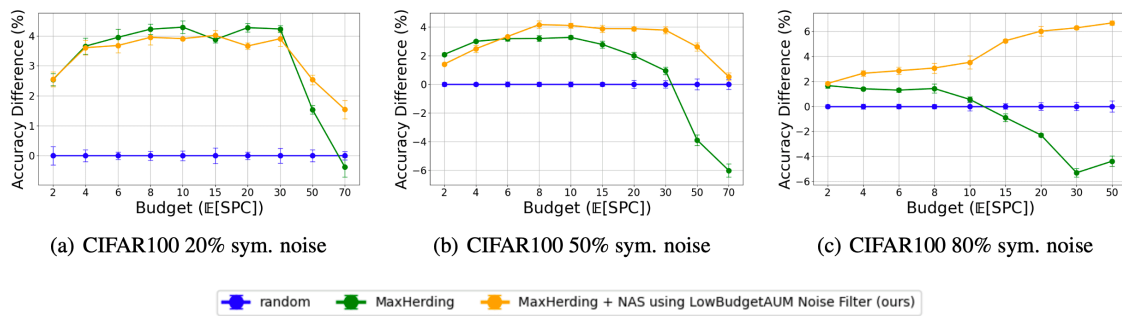


Figure 15. Results of *MaxHerdling* compared to *MaxHerdling* + NAS when using training framework 1.

Appendix E. Clothing1M dataset

Clothing1M^[39] is a real-world large-scale dataset designed for studying learning with noisy labels. It consists of approximately 1 million clothing images collected from online shopping websites, annotated with noisy labels derived from surrounding text. The dataset contains 14 classes and is known to have about 38% estimated label noise. In addition to the noisy set, Clothing1M provides 10k test samples with manually verified labels.

In this experiment, the following modifications were made:

1. Since the LowBudgetAUM algorithm did not predict the noise ratio accurately in preliminary experiments on Clothing1M, we injected the known noise level (38%) as a prior. Concretely, we directly selected the 38% of samples with the lowest AUM scores as noisy, instead of relying solely on

the estimated threshold from LowBudgetAUM. This adjustment improved the stability of the noise filtering step.

2. We found that training on the entire set of labeled samples, including the noisy ones, yielded better performance. Therefore, we trained the model on all labeled samples selected by the active learning procedure without discarding the samples predicted to be noisy.
3. For the NPC-based methods, samples were selected using the regular ProbCover method until the budget reached $4 \mathbb{E}[SPC]$, and afterward the selection switched to the NPC variant. This approach makes sense because LowBudgetAUM may not perform optimally when the budget is extremely low, and it's also held in Figure 8b of the main paper.

For feature extraction, We used DINOv2 pretrained on the LVD-142M dataset. The results obtained under this setup are shown in Fig. 16.

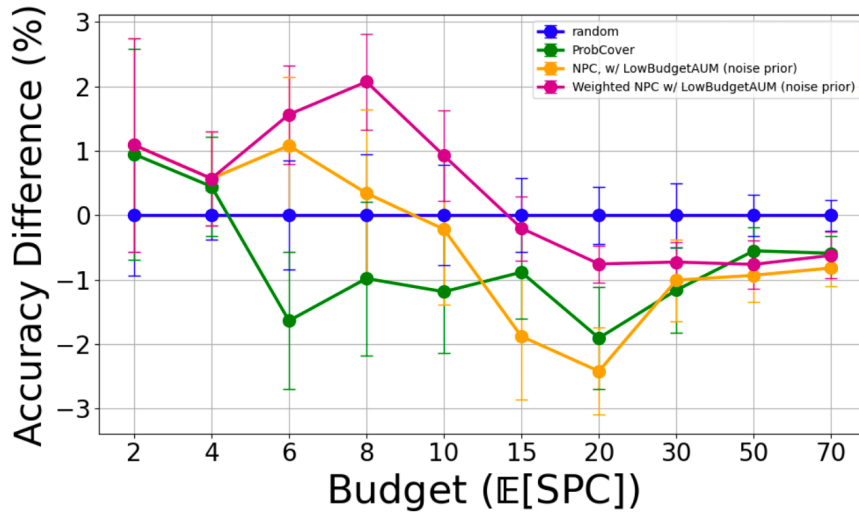


Figure 16. Results on Clothing1M dataset, under the setting described in E, when using training framework 2.

Appendix F. Applying Noise Dropout When the Predicted Noise Is Low

We suggested incorporating the noise dropout practice into NAS in cases where the predicted noise is particularly high. Nevertheless, we observed that when the predicted noise ratios are low, this practice does not affect the results.

In Fig. 17, the performance of NAS is compared to the performance of NAS with noise dropout added, across different levels of symmetric noise. It is evident that while noise dropout resolves the failure of NAS when utilizing *LowBudgetAUM* in the high noise scenario, it has no effect on performance in the low noise scenario.

The numbers above and below the orange and brown lines indicate the predicted noise ratios of *LowBudgetAUM* prior to training. Note that noise dropout is not applied during training but is only used when utilizing *LowBudgetAUM* during NAS query selection.

Examining the predicted noise rates in the 80% symmetric noise scenario, it becomes clear from the plot that while *LowBudgetAUM* predicts nearly all samples to be noisy without noise dropout (orange line), applying noise dropout during query selection (brown line) significantly improves noise prediction before the training. However, the use of noise dropout can be determined automatically during runtime, based on extremely high predicted noise rates. Additionally, this method can be applied when using any noise-filtering algorithms, such as *CrossValidation*.

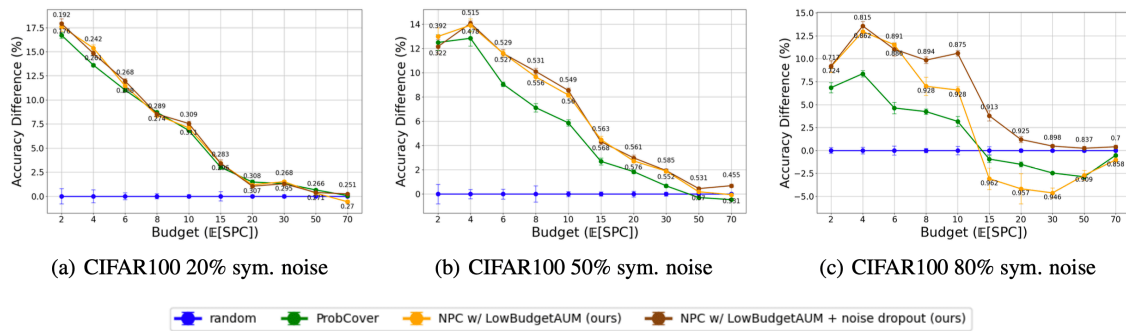


Figure 17. Results of accuracy difference from random strategy, when applying noise dropout as part of NAS given different levels of symmetric noise. The numbers above and under the results of NAS versions presented the predicted noise ratio by *LowBudgetAUM*, when utilizing for noise-filtering before training.

Appendix G. Comparison Between Different Noise Filtering Methods

In the main body of the paper, we presented results using two noise filtering algorithms: a naive algorithm, *CrossValidation*, and a DNN-based algorithm, *LowBudgetAUM*, adapted to the low-budget regime. Here, we compare the performance of various noise filtering algorithms, including *CrossValidation*, *LowBudgetAUM*, and four additional methods—two naive and two DNN-based methods adapted for this setting.

1. Train a kNN classifier on the labeled set and classify as noisy any sample whose majority label among its neighbors differs from its own label. For k , we use $\frac{|L|}{C}$, where C is the number of classes. This simple method shares similarities with the *TopoFilter*^[45] method. We refer to this noise-filtering method as *kNN*.
2. Compute a centroid for each class and classify as noisy any sample whose closest centroid differs from the centroid of its given class. To reduce the influence of noisy samples on the centroids, we use the RANSAC algorithm: For each class, we compute multiple centroids using random subsets of the class and select the one whose subset produces the covariance matrix with the smallest determinant. We refer to this method as *Centroids*.
3. An adapted version of the *DisagreeNet*^[46] method, which uses the consensus between different ensemble checkpoints to classify samples as noisy. We refer to this method as *LowBudgetDisagreeNet*.
4. An adapted version of the *FINE*^[47] method, which classifies samples as noisy based on their low alignment with the first eigenvector of the Gram matrix for their given class. The adaptation involves using SSL representations instead of DNN-based features. We refer to this method as *LowBudgetFINE*.

All these methods use a self-supervised learning (SSL) representation of the dataset. Similar to *LowBudgetAUM*, *LowBudgetDisagreeNet* trains an ensemble of linear models on SSL representations instead of training a DNN on the raw images. Likewise, *LowBudgetFINE* utilizes SSL representations rather than DNN-generated features⁴.

Figure 18 compares the performance of *NPC* variants with different noise filtering algorithms at varying levels of symmetric noise on CIFAR100. Each noise filtering algorithm is used both during query selection (within the inner mechanism of *NPC*) and for noise filtering before training. Additionally, each *NPC* variant is compared with *ProbCover*, which uses the same noise filtering algorithm only prior to training. The different colors in the plots represent the various noise filtering algorithms. Solid lines correspond to *NPC* versions, while dashed lines represent *ProbCover* versions.

The results demonstrate that *NPC* outperforms *ProbCover* for most noise filtering algorithms and budget levels. Furthermore, *LowBudgetAUM* achieves the best results beyond a certain budget, with results for 80% noise further improvable using noise dropout, as shown in Figures 4 and 17(c).

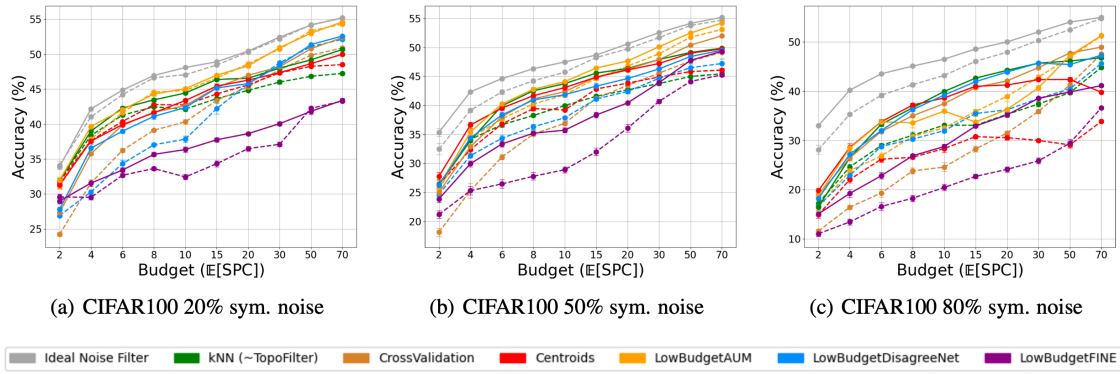


Figure 18. (a) CIFAR100 20% sym. noise (b) CIFAR100 50% sym. noise (c) CIFAR100 80% sym. noise

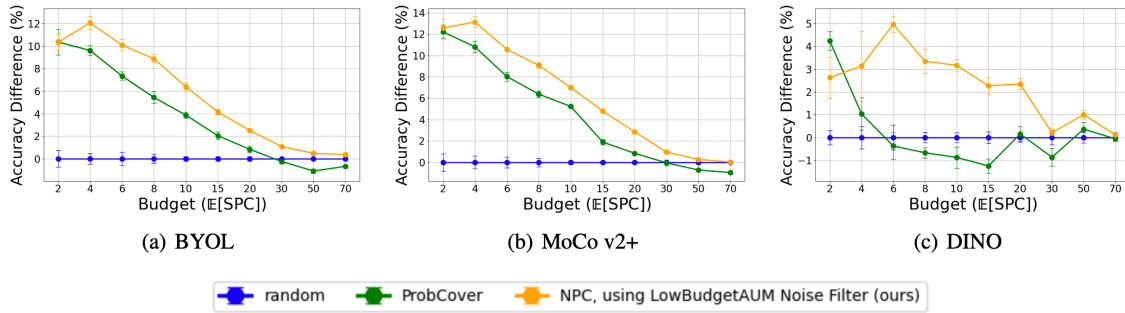


Figure 18. Comparison of different noise filtering methods for CIFAR100 at varying levels of symmetric noise. We used training framework 2 with SimCLR features. The results of NPC in this figure are without the δ updating.

Appendix H. Using Different Feature Spaces

As discussed in this paper, the functionality of NAS relies on the existence of a strong Self-Supervised Learning (SSL) representation of the data. This representation is essential for both the query selection strategy \mathcal{S} , which NAS extends, and the noise filtering algorithm \mathcal{A} that it utilizes.

Figure 19 demonstrates that NPC (the NAS framework when using *ProbCover* as \mathcal{S}) outperforms *ProbCover* on the CIFAR100 dataset with 50% symmetric noise across different feature spaces learned by common SSL algorithms.

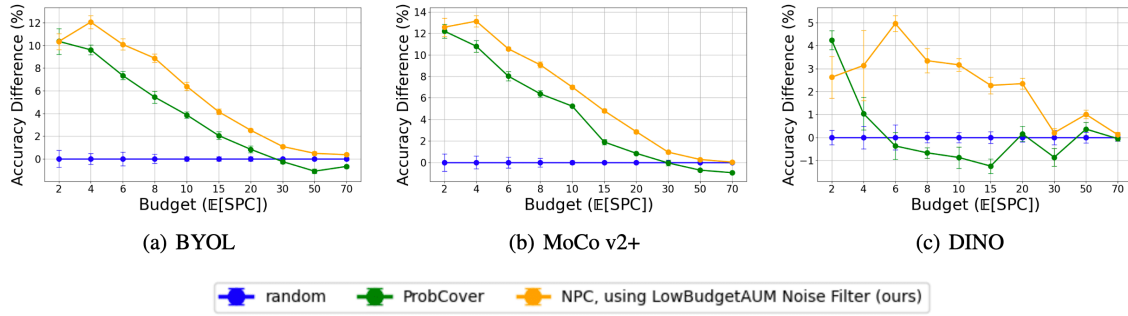


Figure 19. Comparison between *NPC* and *ProbCover* for CIFAR100 with 50% symmetric noise, given different representation spaces. We used training framework 2. The results of *NPC* in this figure are without the δ updating.

Appendix I. Comparison with the *DIRECT* Method

As described in the introduction, the *DIRECT*^[27] method is a query selection strategy that takes into account the presence of noisy labels. Nevertheless, a major part of the *DIRECT* method is intended to address scenarios of extremely imbalanced data (their results present datasets with an imbalance ratio γ of ≈ 0.1 , where γ is the ratio between the number of samples in the smallest class and the number of samples in the largest class).

The issue of imbalanced data is indeed very important but is orthogonal to our research, as *NAS* can integrate strategies like *MaxHerding*^[8], which are designed to handle such scenarios. Additionally, the scoring criterion used by *DIRECT* is more suitable for the high-budget scenario, whereas the strategies *NAS* is most suited to are more tailored to the low-budget regime.

Therefore, we did not consider *DIRECT* as a fair baseline for *NAS* and did not include its performance in our main results. In Figure 20, the results of *DIRECT* in the low-budget regime are compared to *ProbCover* and *NPC*. The dataset used is CIFAR100, under varying levels of symmetric noise when training in framework 2. We utilized the implementation of *DIRECT* from the LabelBench framework^[48] and integrated it into our codebase with minimal necessary changes.

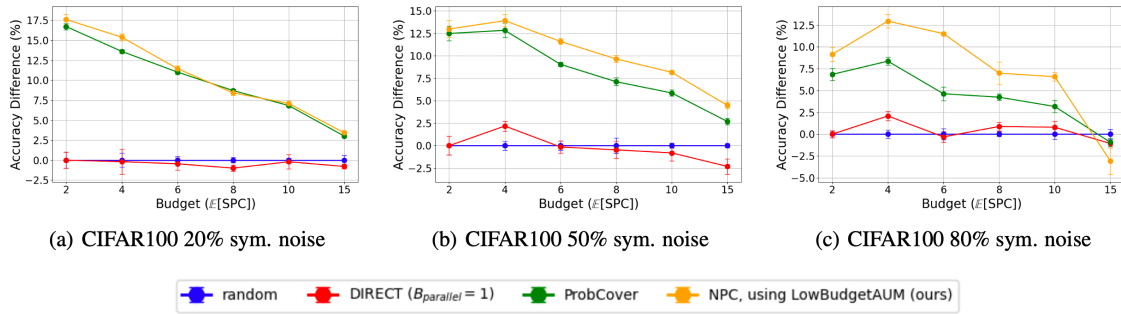


Figure 20. Comparison with the DIRECT method.

Acknowledgments

This work was supported by AFOSR award FA8655-24-1-7006 and the Gatsby Charitable Foundation.

Footnotes

¹ In this discussion, we have not accounted for the annotator, to whom we also send more separate queries as b becomes smaller. For now, we assume that this is not a limiting factor in our setting.

² The noise dropout is only suggested as part of NAS, i.e., during the utilization of *LowBudgetAUM* for query selection, and not when using *LowBudgetAUM* to filter noisy samples before training.

³ As in the *MaxHerding* paper, our experiments involving *MaxHerding* also used a Gaussian kernel with $\sigma = 1$.

⁴ In detail, the original FINE method states: "after warmup training, at every epoch, FINE selects the clean data with the eigenvectors generated from the gram matrices of data predicted to be clean in the previous round, and then the neural networks are trained with them."

References

1. [△]Song Y, Liu Y, Lin Z, Zhou J, Li D, Zhou T, Leung M (2024). "Learning from ai-generated annotations for medical image segmentation." *IEEE Transactions on Consumer Electronics*. pp. 1–1.
2. [△]Scheffer T, Decomain C, Wrobel S (2001). "Active hidden markov models for information extraction." In *International symposium on intelligent data analysis*, pp. 309–318.

3. ^aWang D, Shang Y (2014). "A new active labeling method for deep learning." In 2014 International joint conference on neural networks (IJCNN), pp. 112–119.
4. ^aAsh JT, Zhang C, Krishnamurthy A, Langford J, Agarwal A (2019). "Deep batch active learning by diverse, uncertain gradient lower bounds." *arXiv preprint arXiv:1906.03671*.
5. ^aGhadiri M, Aghaee A, Baghshah MS (2015). "Active distance-based clustering using k-medoids." *arXiv preprint arXiv:1512.03953*.
6. ^{a, b}Hacohen G, Dekel A, Weinshall D (2022). "Active learning on a budget: opposite strategies suit high and low budgets." In *International Conference on Machine Learning*, pp. 8175–8195.
7. ^{a, b, c}Yehuda O, Dekel A, Hacohen G, Weinshall D (2022). "Active learning through a covering lens." *Advances in Neural Information Processing Systems* 35:22354–22367.
8. ^{a, b, c, d, e, f}Bae W, Noh J, Sutherland DJ (2025). "Generalized coverage for more robust low-budget active learning." In *European Conference on Computer Vision*, pp. 318–334.
9. ^{a, b}Chen T, Kornblith S, Norouzi M, Hinton G (2020a). "A simple framework for contrastive learning of visual representations." In *International conference on machine learning*, pp. 1597–1607.
10. ^aChen X, Fan H, Girshick R, He K (2020b). "Improved baselines with momentum contrastive learning." *arXiv preprint arXiv:2003.04297*.
11. ^{a, b}Caron M, Touvron H, Misra I, Jégou H, Mairal J, Bojanowski P, Joulin A (2021). "Emerging properties in self-supervised vision transformers." In *Proceedings of the IEEE/CVF international conference on computer vision*, pp. 9650–9660.
12. ^aHacohen G, Weinshall D (2023). "How to select which active learning strategy is best suited for your specific problem and budget." In *Proceedings of the 37th International Conference on Neural Information Processing Systems*, pp. 13395–13407.
13. ^{a, b}Song H, Kim M, Park D, Shin Y, Lee J (2022). "Learning from noisy labels with deep neural networks: a survey." *IEEE Transactions on Neural Networks and Learning Systems*.
14. ^aSukhbaatar S, Bruna J, Paluri M, Bourdev L, Fergus R (2014). "Training convolutional networks with noisy labels." *arXiv preprint arXiv:1406.2080*.
15. ^aChen X, Gupta A (2015). "Webly supervised learning of convolutional networks." In *Proceedings of the IEEE international conference on computer vision*, pp. 1431–1439.
16. ^aGoldberger J, Ben-Reuven E (2017). "Training deep neural-networks using a noise adaptation layer." In *International conference on learning representations*.

17. ^a ^bGupta G, Sahu AK, Lin W (2019). "Noisy batch active learning with deterministic annealing." *arXiv preprint arXiv:1909.12473*.
18. ^ΔBekker AJ, Goldberger J (2016). "Training deep neural-networks based on unreliable labels." In *2016 IEEE International Conference on Acoustics, Speech and Signal Processing (ICASSP)*, pp. 2682–2686.
19. ^a ^bYao Y, Liu T, Han B, Gong M, Deng J, Niu G, Sugiyama M (2020). "Dual t: reducing estimation error for transition matrix in label-noise learning." *Advances in neural information processing systems* 33:7260–7271.
20. ^ΔArpit D, Jastrzëbski S, Ballas N, Krueger D, Bengio E, Kanwal MS, Maharaj T, Fischer A, Courville A, Bengio Y, et al. (2017). "A closer look at memorization in deep networks." In *International conference on machine learning*, pp. 233–242.
21. ^ΔHan B, Yao Q, Yu X, Niu G, Xu M, Hu W, Tsang I, Sugiyama M (2018). "Co-teaching: robust training of deep neural networks with extremely noisy labels." *Advances in neural information processing systems* 31.
22. ^a ^bPleiss G, Zhang T, Elenberg E, Weinberger KQ (2020). "Identifying mislabeled data using the area under the margin ranking." *Advances in Neural Information Processing Systems* 33, pp. 17044–17056.
23. ^ΔLi J, Socher R, Hoi SC (2020). "Dividemix: learning with noisy labels as semi-supervised learning." *arXiv preprint arXiv:2002.07394*.
24. ^ΔKarim N, Rizve MN, Rahnavard N, Mian A, Shah M (2022). "Unicon: combating label noise through uniform selection and contrastive learning." In *Proceedings of the IEEE/CVF conference on computer vision and pattern recognition*, pp. 9676–9686.
25. ^a ^bXiao R, Dong Y, Wang H, Feng L, Wu R, Chen G, Zhao J (2022). "Promix: combating label noise via maximizing clean sample utility." *arXiv preprint arXiv:2207.10276*.
26. ^ΔChen W, Zhu C, Li M (2023). "Sample prior guided robust model learning to suppress noisy labels." In *Joint European Conference on Machine Learning and Knowledge Discovery in Databases*, pp. 3–19.
27. ^a ^b ^c ^dNuggehalli S, Zhang J, Jain L, Nowak R (2023). "DIRECT: deep active learning under imbalance and label noise." *arXiv preprint arXiv:2312.09196*.
28. ^ΔChakraborty S (2020). "Asking the right questions to the right users: active learning with imperfect oracles." In *Proceedings of the AAAI conference on artificial intelligence*, 34, pp. 3365–3372.
29. ^ΔZhang C, Chaudhuri K (2015). "Active learning from weak and strong labelers." *Advances in Neural Information Processing Systems* 28.
30. ^ΔChen Y, Sankararaman K, Lazaric A, Pirota M, Karamshuk D, Wang Q, Mandyam K, Wang S, Fang H (2022). "Improved adaptive algorithm for scalable active learning with weak labeler." *arXiv preprint arXiv:2211.02223*.

31. ^aLin C, Mausam, Weld D (2016). "Re-active learning: active learning with relabeling." In *Proceedings of the AAAI Conference on Artificial Intelligence*, 30.
32. ^aYounesian T, Zhao Z, Ghiassi A, Birke R, Chen LY (2021). "Qactor: active learning on noisy labels." In *Asian Conference on Machine Learning*, pp. 548–563.
33. ^aTanaka D, Ikami D, Yamasaki T, Aizawa K (2018). "Joint optimization framework for learning with noisy labels." In *Proceedings of the IEEE conference on computer vision and pattern recognition*, pp. 5552–5560.
34. ^aKrizhevsky A, Hinton G, et al. (2009). "Learning multiple layers of features from tiny images."
35. ^aVan Gansbeke W, Vandenhende S, Georgoulis S, Proesmans M, Van Gool L (2020). "Scan: learning to classify images without labels." In *European conference on computer vision*, pp. 268–285.
36. ^aDeng J, Dong W, Socher R, Li L, Li K, Fei-Fei L (2009). "Imagenet: a large-scale hierarchical image database." In *2009 IEEE conference on computer vision and pattern recognition*, pp. 248–255.
37. ^aPatrini G, Rozza A, Krishna Menon A, Nock R, Qu L (2017). "Making deep neural networks robust to label noise: a loss correction approach." In *Proceedings of the IEEE conference on computer vision and pattern recognition*, pp. 1944–1952.
38. ^{a, b}Wei J, Zhu Z, Cheng H, Liu T, Niu G, Liu Y (2021). "Learning with noisy labels revisited: a study using real-world human annotations." *arXiv preprint arXiv:2110.12088*.
39. ^{a, b}Xiao T, Xia T, Yang Y, Huang C, Wang X (2015). "Learning from massive noisy labeled data for image classification." In *Proceedings of the IEEE conference on computer vision and pattern recognition*, pp. 2691–2699.
40. ^{a, b}Sener O, Savarese S (2017). "Active learning for convolutional neural networks: a core-set approach." *arXiv preprint arXiv:1708.00489*.
41. ^aKałuża D, Janusz A, Ślęzak D (2023). "Robust assignment of labels for active learning with sparse and noisy annotations." *arXiv preprint arXiv:2307.14380*.
42. ^aDu J, Ling CX (2010). "Active learning with human-like noisy oracle." In *2010 IEEE international conference on data mining*, pp. 797–802.
43. ^aSchubert M, Riedlinger T, Kahl K, Rottmann M (2023). "Deep active learning with noisy oracle in object detection." *arXiv preprint arXiv:2310.00372*.
44. ^aMunjal P, Hayat N, Hayat M, Sourati J, Khan S (2020). "Towards robust and reproducible active learning using neural networks." *ArXiv abs/2002.09564*.
45. ^aWu P, Zheng S, Goswami M, Metaxas D, Chen C (2020). "A topological filter for learning with label noise." *Advances in neural information processing systems* 33:21382–21393.

46. [^]Shwartz D, Stern U, Weinshall D (2022). "The dynamic of consensus in deep networks and the identification of noisy labels." *arXiv preprint arXiv:2210.00583*.
47. [^]Kim T, Ko J, Choi J, Yun S, et al. (2021). "Fine samples for learning with noisy labels." *Advances in Neural Information Processing Systems* 34, pp. 24137–24149.
48. [^]Zhang J, Chen Y, Canal G, Das AM, Bhatt G, Mussmann S, Zhu Y, Bilmes J, Du SS, Jamieson K, et al. (2024). "LabelBench: a comprehensive framework for benchmarking adaptive label-efficient learning." *Journal of Data-centric Machine Learning Research*.

Declarations

Funding: This work was supported by AFOSR award FA8655-24-1-7006 and the Gatsby Charitable Foundation.

Potential competing interests: No potential competing interests to declare.